

Element Size Effects in Nonlinear Analysis of Reinforced Concrete Beams without Web Reinforcement

Tavio¹

Abstract—A new approach is developed to the nonlinear analysis of reinforced concrete beams without stirrups subjected to a monotonically increasing loading from zero up to the ultimate load. The softening effect of concrete in tension-compression, the tension-stiffening and tension-softening of concrete in tension are all taken into account in the proposed model. The effect of finite element mesh size is investigated by applying the crack band theory (Bazant and Oh, 1983) and taking into account the plastic strain of concrete under tension. A simple procedure for calculating the stress-strain curve of plain concrete under tension was developed and implemented into the nonlinear finite element formulation. The proposed model gives relatively good agreement with the experimental results.

keywords—concrete beams; finite element; mesh size effect; tension-softening; tension-stiffening.

I. INTRODUCTION

The nonlinear finite element method has developed into an important tool for the analysis of the complex concrete structures. This technique is very helpful to understand the formation and propagation of cracks and the mechanism and process of failure. Future development of the nonlinear finite element method lies primarily in the improvements of the constitutive models of materials. Two behavioral models were developed for the analysis of concrete structures subjected to shear: the rotating-angle softened truss model (RA-STM) [1], [2], [3] and the fixed-angle softened truss model (FA-STM) [2],[3], [4], [5]. The FA-STM assumes that cracks will develop along the direction of principal compressive stresses at initial cracking, and the cracks will be “fixed” at this angle thereafter. The advantage of FA-STM over RA-STM was that FA-STM was capable to taking into account the concrete contribution, induced by the shear stresses along the cracks. Nevertheless, the FA-STM overestimate the tension-stiffening of plain concrete and the mesh size effect is not taken into account in the nonlinear finite element analysis based on FA-STM. In this paper, the crack band theory is used to modify the stress-strain curve of cracked plain concrete under tension which revises the overestimation of tension-stiffening. And a plastic tensile strain is introduced into the new model, which is in terms of the finite element mesh size. The crack band theory and the plastic tensile strain can reduce

the numerical error associated with the finite element mesh size.

II. DESCRIPTION OF MODEL

A. Equilibrium Equations

Assuming that the steel bars can resist only axial stresses, then the superposition of concrete stresses and steel stresses as shown in fig. 1 results in

$$\begin{Bmatrix} \sigma_x \\ \sigma_y \\ \tau_{xy} \end{Bmatrix} = \begin{Bmatrix} \sigma_{cx} \\ \sigma_{cy} \\ \tau_{cxy} \end{Bmatrix} + \begin{Bmatrix} \rho_{sx} \sigma_{sx} \\ \rho_{sy} \sigma_{sy} \\ 0 \end{Bmatrix} \quad (1)$$

where,

- σ_x, σ_y = Applied normal stress in the x and y direction, respectively (positive for tension)
- τ_{xy} = Applied shear stress in the x-y coordinate
- σ_{cx}, σ_{cy} = Average normal stress in concrete in the x-y coordinate
- τ_{cxy} = Average shear stress in concrete in the x-y coordinate
- ρ_{sx}, ρ_{sy} = Reinforcement ratios in the x and y-direction, respectively

In the fixed-angle model, the x'-y' coordinate system as shown in Fig. 2 is defined. In this coordinate system, the coordinate x'-y' is the principal coordinate of stresses in concrete at initial cracking. Angle ϕ is the fixed angle between x and x' coordinate.

The transformation of stresses in concrete from the x'-y' coordinate to the x-y coordinate is given as follows:

$$\begin{Bmatrix} \sigma_{cx} \\ \sigma_{cy} \\ \tau_{cxy} \end{Bmatrix} = \begin{bmatrix} c^2 & s^2 & 2cs \\ s^2 & c^2 & -2cs \\ -cs & cs & c^2 - s^2 \end{bmatrix} \begin{Bmatrix} \sigma_{cx'} \\ \sigma_{cy'} \\ \tau_{cx'y'} \end{Bmatrix} \quad (2)$$

where, $c = \cos(-\phi)$ and $s = \sin(-\phi)$. The stresses $\sigma_{cx'}$, $\sigma_{cy'}$ and $\tau_{cx'y'}$ are the stresses in the concrete in x'-y' coordinate.

Manuscript received November 29, 2006; revised November 11, 2007

¹ Tavio is with departement of Civil Engineering, FTSP, Institut Teknologi Sepuluh Nopember, Surabaya, INDONESIA

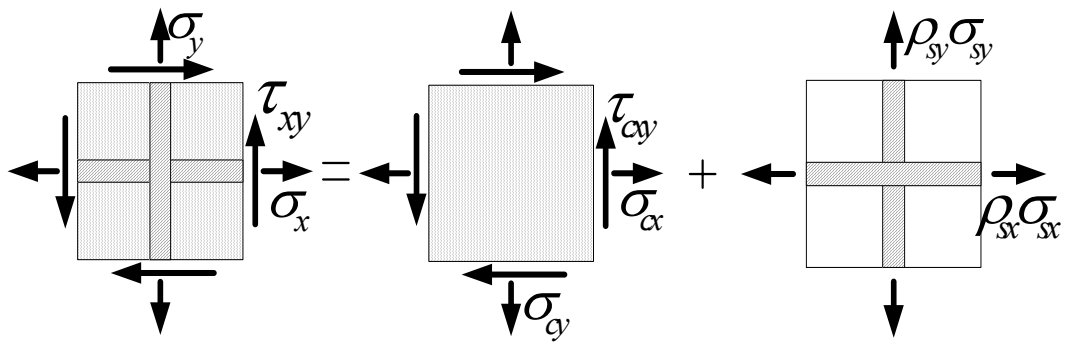


Fig. 1. Superposition of concrete stresses and steel stresses

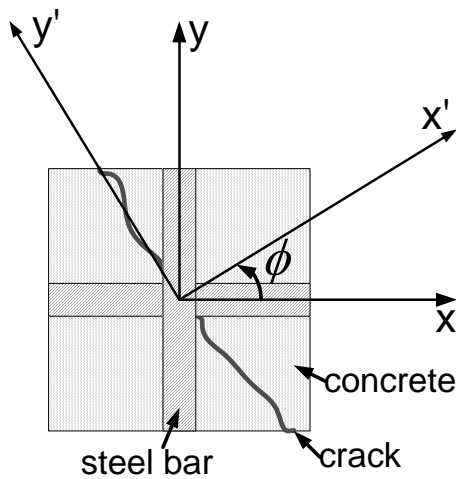


Fig. 2. Definition of coordinate systems and fixed angle

After introducing Eq. 2 into Eq. 1, the final expression for equilibrium condition for reinforced concrete can be obtained as:

$$\begin{Bmatrix} \sigma_x \\ \sigma_y \\ \tau_{xy} \end{Bmatrix} = \begin{bmatrix} c^2 & s^2 & 2cs \\ s^2 & c^2 & -2cs \\ -cs & cs & c^2 - s^2 \end{bmatrix} \begin{Bmatrix} \sigma_{cx'} \\ \sigma_{cy'} \\ \tau_{cx'y'} \end{Bmatrix} + \begin{Bmatrix} \rho_{sx} \sigma_{sx} \\ \rho_{sy} \sigma_{sy} \\ 0 \end{Bmatrix} \quad (3)$$

B. Compatibility equations

Assuming that no slipping occurs between concrete and steel bars, the transformation of the average strains in reinforced concrete from the x-y coordinate to the x'-y' coordinate is given as follows:

$$\begin{Bmatrix} \epsilon_{x'} \\ \epsilon_{y'} \\ \gamma_{x'y'} \end{Bmatrix} = \begin{bmatrix} c^2 & s^2 & cs \\ s^2 & c^2 & -cs \\ -2cs & 2cs & c^2 - s^2 \end{bmatrix} \begin{Bmatrix} \epsilon_x \\ \epsilon_y \\ \gamma_{xy} \end{Bmatrix} \quad (4)$$

where, $c = \cos(\phi)$ and $s = \sin(\phi)$. The strains $\epsilon_{x'}$, $\epsilon_{y'}$, and $\gamma_{x'y'}$ are the strains in the x'-y' coordinate.

C. Cracking criterion

The constitutive relationships of concrete must be guided by an interactive cracking criterion for concrete. A cracking criterion as shown in Fig. 3 is given as follows:

$$\frac{\sigma_{c1}}{f_t} + 0.3 \left(\frac{\sigma_{c2}}{\sigma_{c1}} \right)^2 = 1, \text{ tension-tension} \quad (5a)$$

$$\left(\frac{\sigma_{c1}}{f_t} \right)^3 + \left(\frac{|\sigma_{2c}|}{f'_c} \right) = 1, \text{ tension-compression} \quad (5b)$$

$$\left(\frac{|\sigma_{1c}|}{f'_c} + \frac{|\sigma_{2c}|}{f'_c} \right)^2 - \frac{|\sigma_{2c}|}{f'_c} - 3.65 \frac{|\sigma_{1c}|}{f'_c} = 0, \text{ compression-compression} \quad (5c)$$

where, σ_{1c} and σ_{2c} is the principal stress in concrete.

The uniaxial tensile strength f_t is defined as $0.058 (10 f'_c)^{2/3}$ [10].

As for the cracking envelope under biaxial stress, the Niwa model (1980) derived for the tension-compression domains and the Aoyagi-Yamada model [11] for the domains of tension-tension together with the Kupfer's model [12] for the compression-compression domains are adopted.

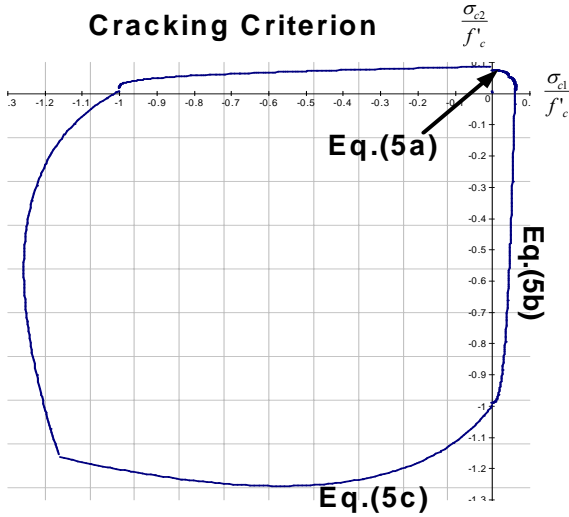


Fig. 3. Cracking surface

D. Constitutive relationships of concrete before initial cracking

Before initial cracking, assuming that the principal direction of stress in concrete is coincide with the principal direction of strain, the constitutive relationships of concrete are given as follows:

$$\sigma_{1c} = E_c \varepsilon_1, \text{ tension} \quad (6a)$$

$$\sigma_{2c} = f'_c \left[2 \left(\frac{\varepsilon_2}{\varepsilon'_c} \right) - \left(\frac{\varepsilon_2}{\varepsilon'_c} \right)^2 \right], \text{ compression} \quad (6b)$$

E. Constitutive relationships of concrete after initial cracking

After initial cracking, the constitutive relationships of concrete are established in the $x'-y'$ coordinate.

F. Concrete in compression-tension

After initial cracking, the stress and strain softening occurs in concrete in compression-tension domains. The average stress-strain curve of concrete in compression [3], [4], [5], [6] as shown in Fig. 4 is expressed as:

$$\sigma_{cy'} = \zeta f'_c \left[2 \left(\frac{\varepsilon_{y'}}{\zeta \varepsilon'_c} \right) - \left(\frac{\varepsilon_{y'}}{\zeta \varepsilon'_c} \right)^2 \right], \varepsilon_{y'} / \zeta \varepsilon'_c \leq 1 \quad (7a)$$

$$\sigma_{cy'} = \zeta f'_c \left[1 - \left(\frac{\varepsilon_{y'} / \zeta \varepsilon'_c - 1}{4 / \zeta - 1} \right)^2 \right], \varepsilon_{y'} / \zeta \varepsilon'_c > 1 \quad (7b)$$

where, f'_c is the cylinder compression strength of concrete; ε'_c is the concrete strain at maximum compressive stress; and ζ is the softening coefficient. In the descending portion of the concrete stress-strain curve the lowest stresses value was taken as $0.2 \zeta f'_c$ to avoid the potential numerical problem in calculation.

In Eq. (7a) and Eq. (7b), the stress-softened coefficient and the strain-softened coefficient are the same value of ζ , which can be expressed conservatively as [4], [5]:

$$\zeta = \frac{5.8}{\sqrt{f'_c}} \frac{1}{\sqrt{1 + \frac{400 \varepsilon_{x'}}{\eta'}}} \quad (8a)$$

$$\eta = \frac{\rho_{sx} f_{syY} - \sigma_y}{\rho_{sy} f_{sxY} - \sigma_x} \quad (8b)$$

$$\eta' = \eta, \eta \leq 1 \quad (8c)$$

$$\eta' = \frac{1}{\eta}, \eta > 1 \quad (8d)$$

where, $\varepsilon_{x'}$ is the tensile strain at x' -direction; ρ_{sx} , ρ_{sy} are the reinforcement ratios in the x and y directions, respectively; f_{sxY} , f_{syY} are the yield stress of steel in the x and y directions, respectively; and σ_x , σ_y are the applied stresses in the x and y directions, respectively. The parameter η' is less than unity.

G. Concrete in shear

The average stress-strain relationship of concrete in shear can be expressed as:

$$\tau_{cx'y'} = \frac{E_{sx'} E_{sy'}}{E_{sx'} + E_{sy'}} \gamma_{x'y'} \quad (9)$$

where, $E_{sx'}$ and $E_{sy'}$ are the secant stiffness of concrete in x' and y' direction respectively. This shear modulus of concrete was proposed by [7].

Transfer of shear forces across the crack surface in reinforced concrete member may result in a large sliding deformation and final failure by shear. Nevertheless, the model is "smeared". It models average responses, without considering the specific contributions of the individual mechanical effects, such as the aggregate interlock and dowel action at the crack location.

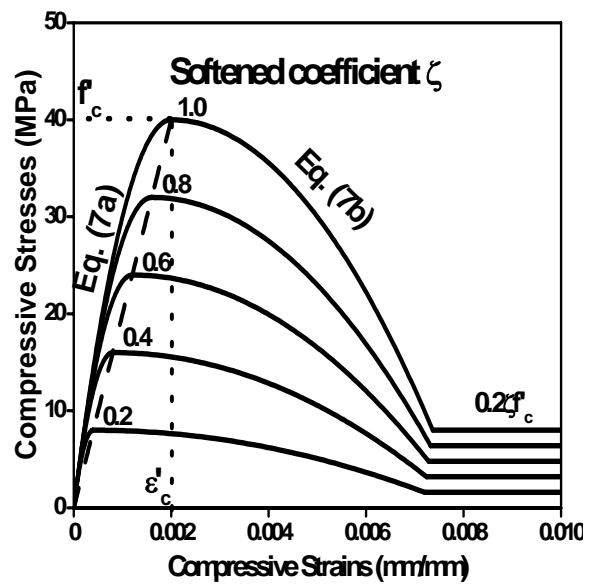


Fig. 4. Softened compressive stress-strain curve of concrete

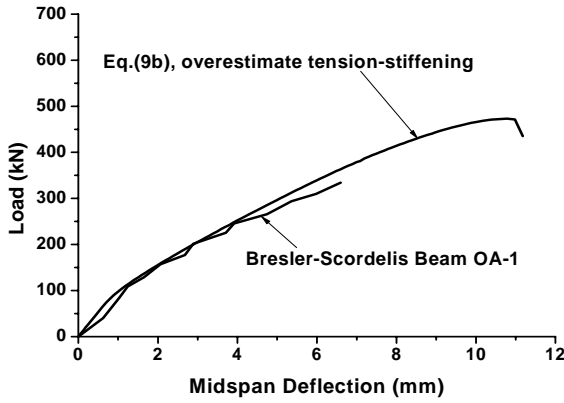


Fig. 5. Load-Deflection estimation using Eq. (9b)

H. Constitutive relationship of steel bar

The stress-strain curve of steel can be modeled by two straight lines [6], [2], [8]. The bilinear model is given as follows:

$$\sigma_s = E_s \varepsilon_s, \varepsilon_s \leq \varepsilon_n \tag{10a}$$

$$\sigma_s = f_y \left[(0.91 - 2B) + (0.02 + 0.25B) \frac{\varepsilon_s}{\varepsilon_y} \right], \varepsilon_s > \varepsilon_n \tag{10b}$$

where, B is a parameter defined as $(1/\rho)(f_{cr}/f_y)^{1.5}$, and ε_n is the average yield strain of mild steel bars embedded in concrete at the beginning of yielding, taken as $\varepsilon_y(0.93 - 2B)$.

I. Concrete in tension

The average stress-strain curve of reinforced concrete in tension can be expressed as:

$$\sigma_{cx'} = E_c \varepsilon_{x'}, \varepsilon_{x'} \leq \varepsilon_{t0} \tag{11a}$$

$$\sigma_{cx'} = f_t \left(\frac{\varepsilon_{t0}}{\varepsilon_{x'} - \varepsilon_p} \right)^{0.4}, \varepsilon_{x'} > (\varepsilon_p + \varepsilon_{t0}), \tag{11b}$$

for reinforced concrete

$$\sigma_{cx'} = f_t, \varepsilon_{t0} < \varepsilon_{x'} \leq (\varepsilon_p + \varepsilon_{t0}) \tag{11c}$$

where, E_c is the modulus of elasticity of concrete; f_t is the uniaxial tensile strength as defined in Eq. (5); ε_{t0} is the cracking strain of concrete, which equals to $\frac{f_t}{E_c}$; ε_p

is the plastic strain of concrete under tension. In Belarbi and Hsu's model [6], the value of ε_p was set to be zero.

Eq. (11b) can well estimate the tension-stiffening of reinforced concrete under tension. However, Eq. (11b) may overestimate the tension-stiffening and underestimate the tension-softening of plain concrete. A numerical result using Eq. (11b) is compared with the experimental result reported by Bresler and Scordelis (1963) in Fig. 5, which shows that the Eq. (11b) may overestimate the ultimate load of the beam without stirrups. Because the cracks in plain concrete can grow without the restriction by the reinforcing bars, the tensile stress in plain concrete can

drop faster than in reinforced concrete. Thus a new approach is proposed to predict the behavior of plain concrete under tension, which can be expressed as:

$$\sigma_{cx'} = E_c \varepsilon_{x'}, \varepsilon_{x'} \leq \varepsilon_t \tag{12a}$$

$$\sigma_{cx'} = f_t \left(\frac{\varepsilon_{t0}}{\varepsilon_{x'} - \varepsilon_p} \right)^\beta, \varepsilon_{x'} > (\varepsilon_p + \varepsilon_{t0}), \tag{12b}$$

for plain concrete

$$\sigma_{cx'} = f_t, \varepsilon_{t0} < \varepsilon_{x'} \leq (\varepsilon_p + \varepsilon_{t0}) \tag{12c}$$

where, E_c is the modulus of elasticity of concrete; f_t is the uniaxial tensile strength as defined in Eq. (5); ε_{t0} is the cracking strain of concrete, which equals to $\frac{f_t}{E_c}$.

In this proposed model, the parameter β used in Eq. (12b) is calculated based on crack band theory. In the crack band theory, the basic criterion is that of energy release needed to create the crack surface. The fracture energy, G_f is the energy consumed in the formation and opening of all microcracks per unit area, which was defined by Bazant as:

$$G_f = w_c \int_{\sigma_{cx'}=f_t}^0 \sigma_{cx'} d\varepsilon_f = w_c W \tag{13}$$

in which, w_c is the effective width of the crack band over which the microcracks are assumed to be uniformly spread; σ_t is the tension stress in plain concrete; ε_f is the fracture strain that is the additional strain caused by the opening of microcracks.

As shown in Fig. 6, the value of W is the hatched area. Substituting for $\sigma_{cx'}$ from Eq. (12a) and Eq. (12b), the value of W can be

$$\begin{aligned} W &= 0.5 f_t \varepsilon_{t0} + \int_{\varepsilon_{t0}}^\infty \sigma_{cx'} d\varepsilon_{cx'} \\ &= 0.5 f_t \varepsilon_{t0} + \frac{f_t \varepsilon_{t0}}{\beta - 1} \\ &= \frac{G_f}{w_c} \end{aligned} \tag{14}$$

So the value of β can be defined as a function of fracture energy G_f , the tensile strength f_t , ε_{t0} and the effective width of crack band w_c . In finite element analysis, the effective width of crack band can be replaced by the finite element size h [9]. Thus, the equation of β is

$$\beta = \frac{f_t \varepsilon_{t0} h + 2G_f}{2G_f - f_t \varepsilon_{t0} h} \tag{15}$$

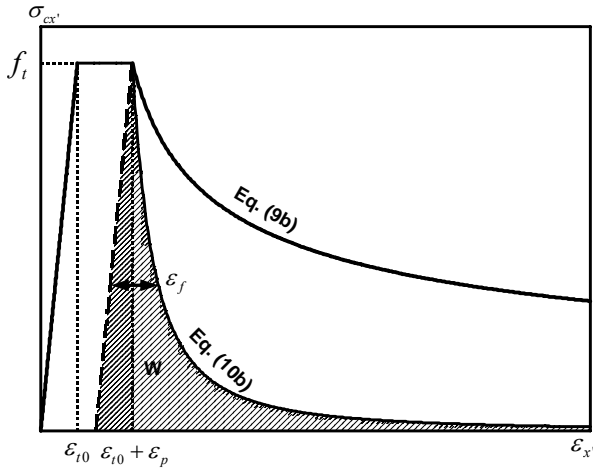


Fig. 6. Stress-Strain Curves of Concrete under Tension

The fracture energy, G_f is a material parameter. Referring to reference [9] proposed an empirical function for G_f of plain concrete as:

$$G_f = (2.72 + 0.0214 f_t) f_t^2 \frac{d_a}{E_c} \quad (16)$$

in which, d_a is the aggregate size in concrete.

By implementing Eq. (12b) into the nonlinear finite element analysis of reinforced concrete beams without stirrups and assuming $\epsilon_p = 0$, the numerical result is compared with the experimental result reported by Bresler and Scordelis (1963) in Fig. 7. It is found that the numerical result underestimate the ultimate load. The similar results are found in the other Bresler and Scordelis beams without stirrups.

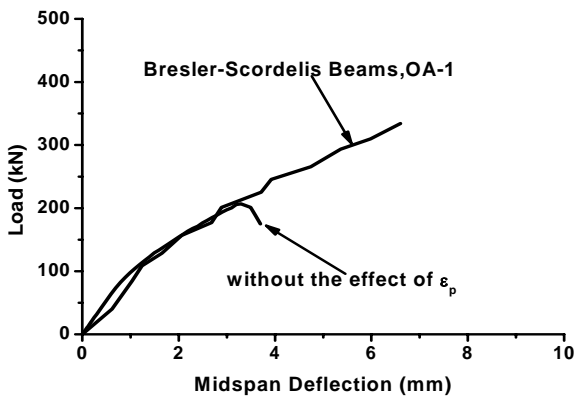


Fig. 7. Load-Deflection without the Effect of ϵ_p

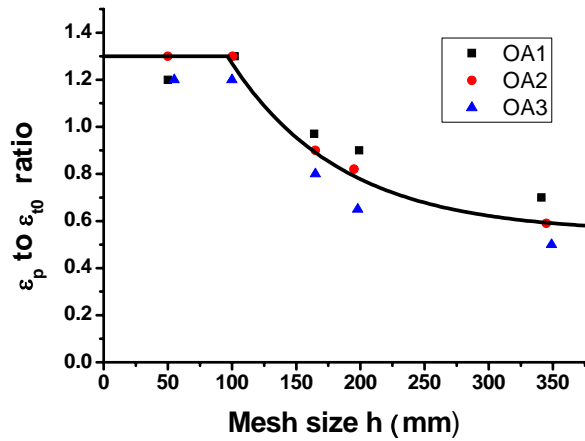


Fig. 8. Plastic tensile strain, ϵ_p vs. width of element, h

From the present research work, it is found that the underestimation of the ultimate load can be revised by implementing the plastic strain ϵ_p into the model of concrete under tension as in Eq. (11c) and Eq (12c). Furthermore, the value of ϵ_p is affected by the finite element size. To obtain the function of ϵ_p , three reinforced concrete beams without stirrups reported by Bresler and Scordelis (1963) were analyzed. The series of beams own of the high quality of the testing and results. For each of the beams, five types of mesh size were used in the finite element analysis. The details are shown in Table 1.

For each mesh configuration, the value of ϵ_p was adjusted so that the computed ultimate load was close to the experimental ultimate load. The results are presented in Table 2. After determining the best value of ϵ_p for each mesh size h , the variation of ϵ_p with respect to the element width is plotted in Fig. 8. A regression analysis of the results leads to the following exponential equation:

$$\epsilon_p = (0.55 + 2.27 e^{-\frac{1}{70.0}}) \epsilon_{t0} \quad (17)$$

in which, h is the width of the element (mm) (for non-square elements: $h = \sqrt{A}$, where A is the element area). If ϵ_p is larger than $1.4\epsilon_{t0}$, than $\epsilon_p = 1.4\epsilon_{t0}$. Based on this formula, the value of ϵ_p decreases with an increase in the value of h .

TABLE 1
DETAILS OF BRESLER-SCORDELIS BEAMS

Beam		mm	$b \times h$, mm	Span, mm	f'_c , MPa	Bottom reinforcement	a/d
OA-1	Mesh Size 1	50 x 50	305 x 552	3660	22.6	4 No. 9	3.32
	Mesh Size 2	100 x 100					
	Mesh Size 3	150 x 180					
	Mesh Size 4	220 x 150					
	Mesh Size 5	420 x 280					
OA-2	Mesh Size 1	50 x 50	305 x 552	4570	23.7	5 No. 9	4.14
	Mesh Size 2	100 x 100					
	Mesh Size 3	150 x 150					
	Mesh Size 4	220 x 150					
	Mesh Size 5	420 x 180					
OA-3	Mesh Size 1	50 x 50	305 x 552	6400	37.6	6 No. 9	5.80
	Mesh Size 2	100 x 100					
	Mesh Size 3	150 x 150					
	Mesh Size 4	220 x 150					
	Mesh Size 5	420 x 280					

TABLE 2
OPTIMUM VALUE OF ϵ_p FOR DIFFERENT MESH SIZES

Size of Element (mm)	The optimum value of plastic strain ϵ_p ($\times \epsilon_{t0}$)		
	OA-1	OA-2	OA-3
50 x 50	2.20	2.30	2.20
100 x 100	2.30	2.30	2.20
150 x 150	1.97	1.90	1.80
220 x 150	1.90	1.82	1.65
420 x 280	1.70	1.59	1.50

TABLE 3
DETAILS OF TSUCHIYA BEAMS (SERIES 1)

Beam		mm	$b \times h$, mm	Span, mm	f'_c , MPa	f_y , MPa	a/d
No.1	Mesh Size 1	50 x 40	150 x 300	780	69.5	711	3.0
	Mesh Size 2	100 x 80					
	Mesh Size 3	200 x 100					
No.2	Mesh Size 1	50 x 40	150 x 300	780	29.4	711	3.0
	Mesh Size 2	100 x 80					
	Mesh Size 3	200 x 100					
No.4	Mesh Size 1	50 x 40	150 x 300	780	29.4	333	3.0
	Mesh Size 2	100 x 80					
	Mesh Size 3	200 x 100					
No.7	Mesh Size 1	50 x 40	150 x 300	780	69.5	363	3.5
	Mesh Size 2	100 x 80					
	Mesh Size 3	200 x 100					

III. COMPARISON BETWEEN NUMERICAL ANALYSIS AND EXPERIMENTAL DATA

To verify the reliability of the proposed method, 7 beams were analyzed. The comparisons between the proposed model and the experimental results of Bresler-Scordelis beams are shown in Fig. 9. The figure shows the relationship between the load and midspan deflection. The numerical results are also compared with Tsuchiya's beams (series 1, 2002)[10]. The details of the beams are listed in Table 3. The comparisons of the load-deflection curves are shown in Fig. 10. All the

compared beams are slender beams. In this figure, it is found that the load-displacement curves calculated by the model with considering the finite element size effect can predict the load-deflection curve of concrete beams without stirrups. The numerical results give reasonably good agreement with the experimental results of normal concrete slender beams including OA1, OA2, OA3, No. 2 and No. 4 beams. However, the finite element analysis for the high-strength slender beams (OA1 and OA7) does not give good enough agreement, especially for the load-deflection curve of beam No.7 near the peak load point. It may be because Eq. (17) is an

empirical equation got from the experimental result of normal beams. The parameters in Eq. (17) may be in terms of the material properties.

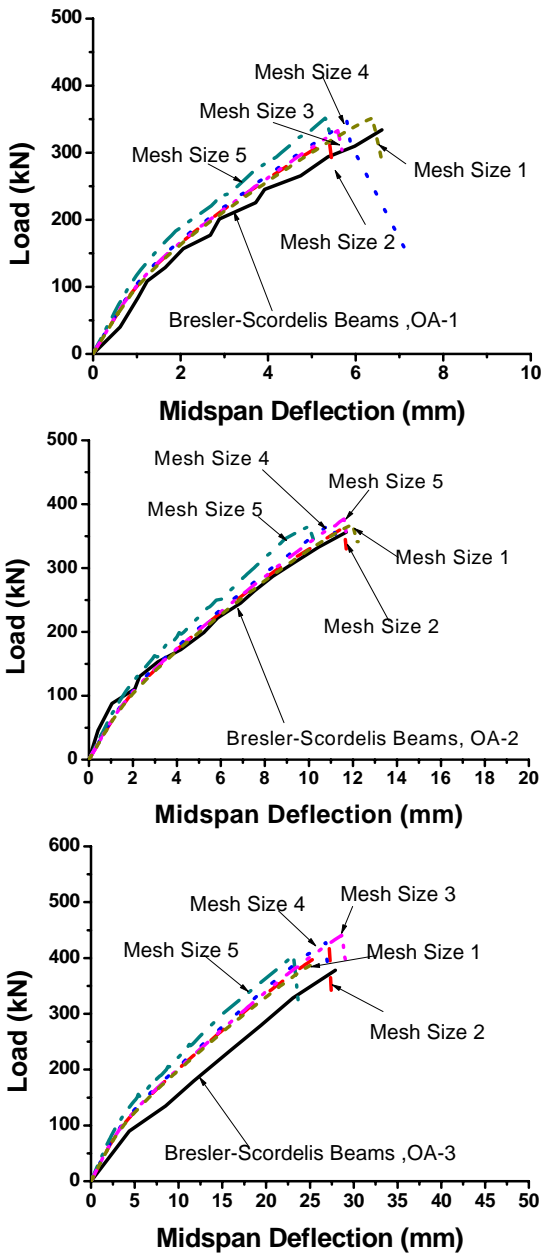


Fig. 9. Comparison of results of analysis for Bresler-Scordelis Beams.

IV. CONCLUSIONS

In this paper a new approach is developed to do the nonlinear analysis of concrete slender beams without web reinforcement. The crack band theory is applied in this approach to decide the stress-strain relationship of cracked concrete under tension. And a function for the plastic tensile strain is established that is a function of the finite element size. The crack band theory and the plastic tensile strain can reduce the numerical error associated with the mesh size. The calculated deflections agreed with the experimental results reasonably, thus making it possible to model the concrete beams without stirrups with relatively large finite element mesh size.

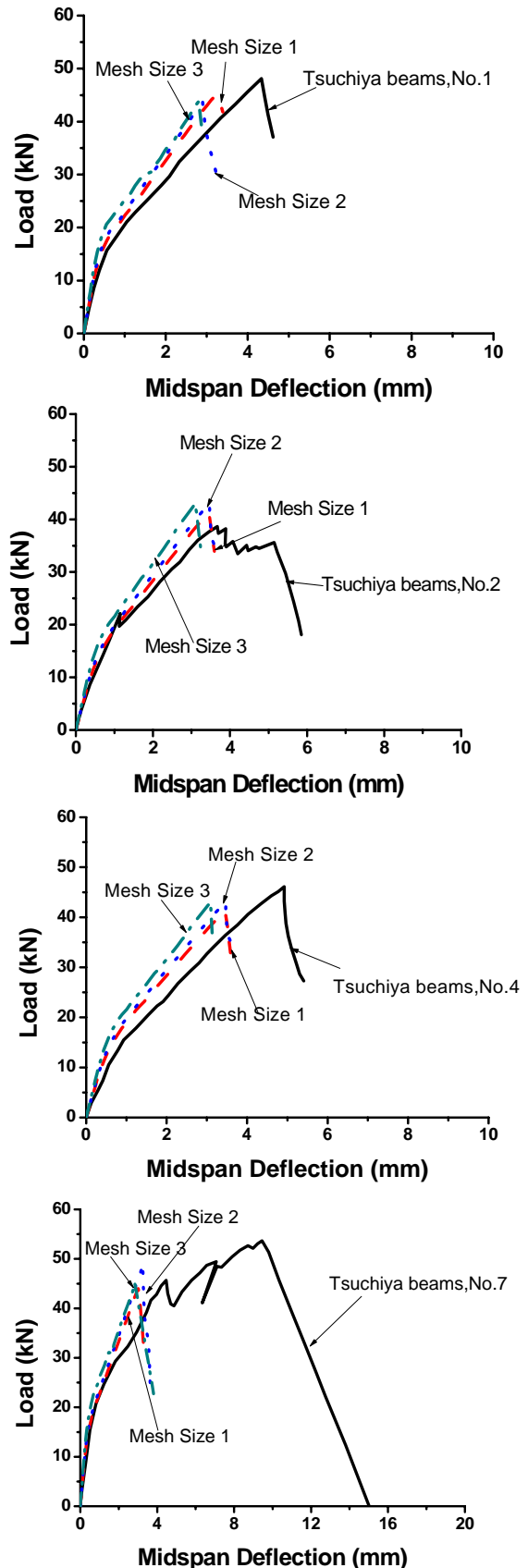


Fig. 10. Comparison of results of analysis for Tsuchiya's Beams.

V. REFERENCES

- [1] Hsu, T. T. C., "Nonlinear Analysis of Concrete Membrane Elements," *Struct. J. ACI*, V. 88, No. 5, pp. 552-561. 1991.
- [2] Pang, X. B.; and Hsu, T. T. C., "Behavior of Reinforced Concrete Membrane Elements in Shear," *Struc. J. ACI*, V. 92, No. 6, pp. 665-679. 1995.

- [3] Hsu, T. T. C., *Unified Theory of Reinforced Concrete*, Boca Raton, FL: CRC Press; 1993.
- [4] Hsu, T. T. C., and Zhang, L. X., "Nonlinear Analysis of Membrane Elements by Fixed-Angle Softened-Truss Model," *Struct. J. ACI*, V. 94, No.5, pp. 483-492. 1997.
- [5] Zhang L. X.; and Hsu, T. T. C., "Behavior and Analysis of 100 MPa Concrete Membrane Elements," *J. Struct. Eng. ASCE*, V. 124, No. 1, pp. 24-34. 1998.
- [6] Belarbi, A.; and Hsu, T. T. C., "Constitutive Laws of Concrete in Tension and Reinforcing Bars Stiffened by Concrete," *Struct. J. ACI*, V. 91, No. 4, pp. 465-474. 1994.
- [7] Vecchio, F. J.; and Collins, M. P., "Nonlinear Finite Element Analysis of Reinforced Concrete Membranes," *ACI Struct. J.*, Vol. 86, No. 1, pp. 26-35. 1989.
- [8] Pang, X. B; and Hsu, T. T. C., "Fixed-Angle Softened-Truss Model for Reinforced Concrete," *Struct. J. ACI*, V. 93, No. 2, pp. 197-207. 1996.
- [9] Bazant, Z. P.; and Oh, B. H. "Crack Band Theory for Fracture of Concrete," *Mater. Struct.*, Vol. 16, No. 93, pp. 155-177.
- [10] Tsuchiya, S.; Mishima, T.; and Maekawa, K., "Shear Failure and Numerical Performance Evaluation of RC Beam Members with High-Strength Materials," *J. Mater. Conc. Struct. Pavements, JSCE*, No. 697/V-54, pp. 65-84. 2002.
- [11] Aoyagi, Y.; and Yamada, K. "Strength and Deformation Characteristics of Reinforced Concrete Shell Elements Subjected to In-plane Forces," *Proc. of JSCE*, No. 331, pp. 167-180. 1983.
- [12] Kupfer, H. B.; Hilsdorf, H. K., and Rusch, H., "Behavior of Concrete under Biaxial Stresses," *J. ACI*, V. 66, No. 8, pp. 656-666. 1969.
- [1] G. Brandli and M. Dick, "Alternating current fed power supply," U.S. Patent 4 084 217, Nov. 4, 1978.